Production of Carbon Nanotubes by PECVD and Their Applications to Supercapacitors

Burak Caglar

Prof. Enric Bertran and Dr. Eric Jover, Department of Applied Physics and Optics and Institute Nanoscience and Nanotechnology, IN2UB, Universitat de Barcelona, C/ Marti i Franques, 1, 08028, Barcelona, Spain

***Abstract*— Plasma enhanced chemical vapor deposition (PECVD) is a versatile technique to obtain vertically dense-aligned carbon nanotubes (CNTs) at lower temperatures than chemical vapor deposition (CVD). In this work, we used magnetron sputtering to deposit iron layer as a catalyst on silicon wafers. After that, radio frequency (rf) assisted PECVD reactor was used to grow CNTs. They were treated with water plasma and finally covered by MnO_2 as dielectric layer in order to use CNTs as electrode for supercapacitors. Optimization of annealing time, reaction time and temperature, water plasma time and MnO_2 deposition time were performed to find appropriate conditions to improve the characteristics of supercapacitors. SEM (Scanning Electron Microscopy), TEM (Transmission Electron Microscopy), AFM (Atomic Force Microscopy) and Raman spectroscopy were used to characterize obtained electrodes.**

***Index Terms*—5.Nanostructured Materials: Plasma Enhanced Chemical Vapor Deposition (PECVD), Carbon Nanotubes (CNTs), Magnetron Sputtering, Supercapacitor**

I. INTRODUCTION

NANOTECHNOLOGY is the construction and use of functional structures designed from atomic or molecular scale with at least one characteristic dimension in nanometer range. Their size allows them to exhibit novel and significantly improved physical, chemical, and biological properties because of their size. When characteristic structural features are intermediate between isolated atoms and bulk materials in the range of about one to 100 nanometers, the objects often display physical attributes substantially different from those displayed by either atoms or bulk materials [1]. Nanotechnology is going to change the world and the way we live, creating new scientific applications that are smaller, faster, stronger, safer and more reliable [2]. As impressive as nanotechnology might be, there are also potential disadvantages; potential mass poisoning over a period of time or incredibly small particles that may very well cause eventual health problems in the consumers that use them [3].

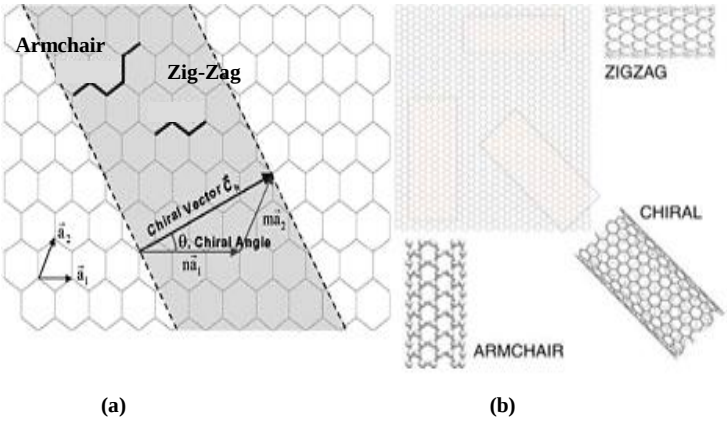

***Fig. 1.** (a) Schematic diagram showing how a hexagonal sheet of graphite is 'rolled' to form a carbon nanotube (b) Illustrations of the atomic structure of an armchair, a zig-zag and a chiral nanotube [4].*

A. Carbon Nanotubes

Carbon nanotubes are built from sp^2 carbon units and consist of honeycomb lattices and are a seamless structure. They are tubular having a diameter of a few nanometers (b) but lengths of many microns. MWCNTs are closed graphite tubules rolled like a graphite sheet. Diameters usually range between *2* and *25 nm* and single-walled carbon nanotubes' (SWCNT) are made of a single seamlessly rolled graphite sheet with a typical diameter of about *1.4 nm* which is similar to a buckyball (C60). They have a tendency to form in bundles which are parallel in contact and consist of tens to hundreds of nanotubes. Depending on how the graphene walls of the nanotube are rolled together they can result in an armchair, zigzag or chiral shapes (fig.1b). These groups are distinguished by their unit cells which are determined by the chiral vector given by the equation: $C_h = na_1 + ma_2$ where a_1 and a_2 are unit vectors in the two-dimensional hexagonal lattice, and n and m are integers as seen in fig.1a. Another important parameter is the chiral angle, which is the angle between C_h and a_1. When n = m and the chiral angle is 30^0 degrees it is known as an armchair type. When m or n are zero and the chiral angle is equal to zero the nanotube is known as *zigzag*. Chiral nanotubes are therefore when the chiral angles are between 0^o and 30^o.

a. Properties

Carbon nanotubes (CNTs) are unique nanostructures which are known to have remarkable electronic and mechanical properties. These characteristics have sparked great interest in their possible uses for nano-electronic and nano-mechanical devices. CNTs have elastic modulus of greater than *1 TPa* (that of a diamond is *1.2 TPa*) and strength *10–100* times higher than the strongest steel at a fraction of the weight. They can conduct electric current carrying capacity *1000* times higher than copper wires. The nanotubes were found to have an extremely large breaking strain which decreased with temperature [4]. In the π-tight-binding model within the zone-folding scheme, one third of the nanotubes are metallic and two thirds are semiconducting depending on their indices (*n*, *m*) [5]. On the other hand, carbon nanotubes that arise during the production process may induce oxidative stress and prominent pulmonary inflammation [6]. Studies collectively show that regardless of the process by which CNTs were synthesized and the types and amounts of metals they contained, CNTs were capable of producing inflammation, epithelioid granulomas (microscopic nodules), fibrosis, and biochemical/toxicological changes in the lungs [7]. The needle-like fiber shape of CNTs, similar to asbestos fibers, raises fears that widespread use of carbon nanotubes may lead to mesothelioma, cancer of the lining of the lungs often caused by exposure to asbestos [8]. Although further research is required, results presented today clearly demonstrate that, under certain conditions, especially those involving chronic exposure, carbon nanotubes can pose a serious risk to human health. Therefore, their use has to assess the whole life cycle of the product and its proper disposal.

b. Applications

The unique properties of both the single-walled and multi-walled varieties of carbon nanotubes have led to several studies in modern physics, resulting in applications in a wide variety of materials and devices [9]. CNTs' small size with larger surface area, high sensitivity and fast response to gas molecules and good reversibility at room temperature enable them as a gas molecule sensors, high electrical conductivity, and chemical stability make them good electron emitters, carbon nanotubes are also being considered for energy storage and production because of their small dimensions, a smooth surface topology, and perfect surface specificity [4], they are also used in scanning probe tips or as a composite on airplane wings and fuselages.

c. Supercapacitors

Electrochemical double-layer capacitors, also known as supercapacitors or ultracapacitors, are electrical storage devices, which have a relatively high energy storage density simultaneously with a high power density.

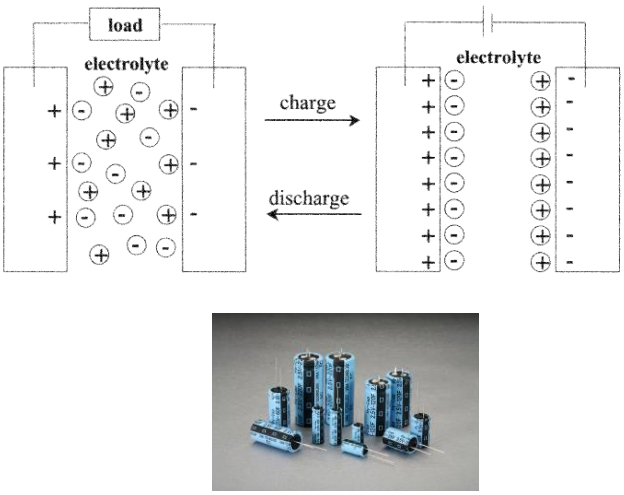

Fig. 2. *Electrochemical double-layer capacitors [11]*

Recent developments in basic technology, materials and manufacturability have made supercapacitors an imperative tool for short term energy storage in power electronics. Supercapacitors consist of two electrodes immersed in or impregnated with an electrolyte solution with a semi-permeable membrane serving as a separator that prevents electrical contact between the two electrodes, but which allows for ionic diffusion (fig. 2). When an electric potential is applied to the electrodes, a potential difference is created at the electrode-electrolyte interface. This electrostatic interface consists of a double layer between ions in the electrolyte and the electronic charges on the electrode.

There are several reasons why CNT-based electrodes perform prosperously in supercapacitors. Nanotubes have high conductivity, large surface area (*1* to *>2000* m^2/g), good corrosion resistance, high temperature stability, percolated pore structure, and can be functionalized to optimize their properties [10].

Multi-walled (MWCNTs) and single-walled carbon nanotubes (SWCNTs) have been already proposed as electrode materials for supercapacitors. Different values of specific capacitance depend mainly on the kind and purity of samples. Generally, for highly purified nanotubes, *i.e. without other carbon forms and residual catalyst,* specific capacitance varies from *15* to *80* F/g of nanotubular material. Pure carbon nanotubes possess a very high surface area from *120* to *400* m^2/g due to their highly mesoporous character connected with entanglement and/or presence of central canal. Generally, the more graphitized nanotubes the smaller values of capacitance. On the other hand, presence of defects causes an increase in the ability of accumulating of charges. It is well known that charging of electrical double layer proceeds mainly in the access of solvated ions through micropores of electrode whereas mesopores play an important transportation role as well as, adsorption. Hence, enhancement of nanotubes

microporosity is of great interest for supercapacitor application but also for other electrochemical application (hydrogen storage, support for catalyst). An improvement of capacitance can be realized by increasing the electrode surface area of nanotubes or by pseudofaradaic effects obtained by the addition of special oxides or conducting polymers [12]. Manganese can be present in various valence states, and its oxides are promising candidates for electrochemical capacitors (ECs) because of their low cost and being environmentally friendly [13]. Because of these several reasons, in this work, it was decided to deposit MnO_2 onto the obtained CNTs in order to improve their behavior.

B. Production Methods

a. CVD (Chemical Vapor Deposition)

The CVD method (fig.3) uses a carbon source in the gas phase and plasma or a resistively heated coil, to transfer the energy to the gaseous carbon molecule. The commonly used carbon sources are CH_4, CO_2 and C_2H_2. The process temperature cracks the molecule into atomic carbon. The carbon then diffuses toward the substrate, which is heated and coated with a catalyst (usually a first row transition metal such as Ni, Fe, or Co) and binds to it [14]. CNTs are formed in this procedure if the proper parameters are maintained such as the temperature and the pressure of operation, the volume and concentration of carbon sources, the size and the pretreatment of metallic catalyst, and the time of reaction [4].

Control over the diameter as well as the growth rate of the nanotubes is achieved by CVD method. Use of an appropriate metal catalyst permits the preferential growth of SWCNTs rather than MWCNTs. CVD synthesis of nanotubes is essentially a two-step process, consisting of a catalyst preparation step followed by the actual synthesis of the nanotube. The catalyst is generally prepared by sputtering a transition metal onto a substrate and then using etching by chemicals such as ammonia or thermal annealing to induce the nucleation of catalyst particles. Thermal annealing results in metal cluster formation on the substrate, from which the nanotubes grow. The temperature for the synthesis of nanotubes by CVD is generally in the *650-900°C* range [14].

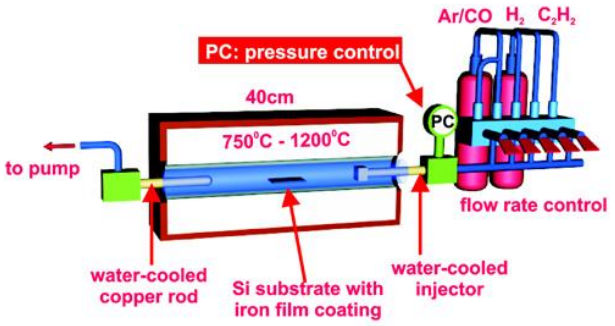

Fig. 3. *Schematic of CVD [15]*

To eliminate impurities formed during the process such as graphite compounds, amorphous carbon, fullerenes, coal and metal nanoparticle, purification is needed. This is achieved by oxidative treatments in the gaseous phase, liquid phase, acid treatment, micro filtration, thermal treatment and ultrasound methods [4].

b. Arc Discharge

The arc discharge method (fig.4), initially used for producing C60 fullerenes, is the most common and perhaps easiest way to produce CNTs as it is rather simple to undertake. However, it is a technique that produces a mixture of components and requires separating nanotubes from the soot and the catalytic metals present in the crude product [16].

In this method an electric arc discharge is generated between two graphite electrodes under inert atmosphere of helium or argon. A very high temperature is obtained which allows the sublimation of the carbon. For the carbon nanotubes to be obtained, purification by gasification with oxygen or carbon dioxide is needed. For single wall nanotubes to be obtained a metal catalyst is needed. Process parameters involve small gaps between electrodes *(~1 mm*), high current (*100 A*), plasma between the electrode at about *4000 K* and voltage range (*30–35 V*) under specified electrode dimensions [4].

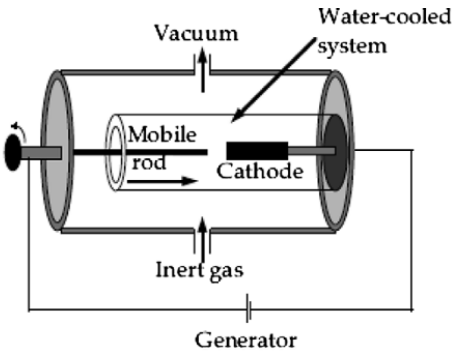

Fig. 4. *Arc Discharge [4]*

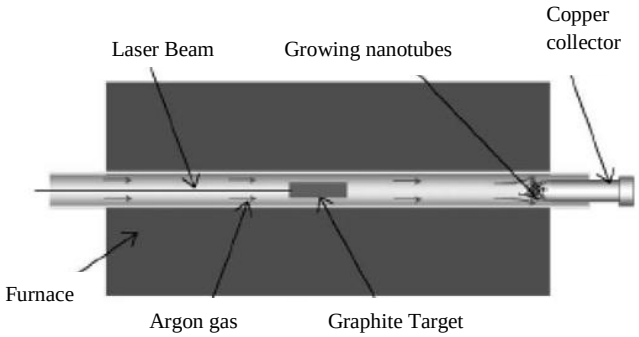

Fig. 5. *Laser Ablation [4]*

c. Laser Ablation

A pulsed or continuous laser (fig.5) is used to vaporize a graphite target in an oven at *1200^oC*. The oven is filled with helium or argon gas in order to keep the pressure at *500Torr* (*6,7x10^{4}Pa*). A hot vapor plume forms, then expands and cools rapidly.

As the vaporized species cool, small carbon molecules and atoms quickly condense to form larger clusters, possibly including fullerenes. The catalysts also begin to condense, but more slowly at first, and attach to carbon clusters and prevent their closing into cage structures. Catalysts may even open cage structures when they attach to them. From these initial clusters, tubular molecules grow into SWCNTs until the catalyst particles become too large, or until conditions have cooled sufficiently that carbon no longer can diffuse through or over the surface of the catalyst particles [14].

d. PECVD (Plasma Enhanced Chemical Vapor Deposition)

The plasma-enhanced CVD (PECVD) method involves a glow discharge in a chamber or a reaction furnace through a high-frequency voltage applied to both the electrodes. Fig. 6 shows a schematic diagram of a typical PECVD apparatus with a parallel plate electrode structure. A substrate is placed on the grounded electrode. In order to form a uniform film, the reaction gas is supplied from the opposite plate. Catalytic metals such as Fe, Ni, and Co are used on a Si or SiO_2 substrate using thermal CVD or sputtering. After the nanoscopic fine metal particles are formed, the CNTs grow on the metal particles on the substrate by the glow discharge generated from a high-frequency power source. A carbon-containing gas, such as C_2H_2, CH_4, C_2H_4, C_2H_6, or CO is supplied to the chamber during the discharge. The catalyst has a strong effect on the nanotube diameter, growth rate, wall thickness, morphology, and microstructure [14].

In ordinary CVD processes, films are formed purely through thermochemical reactions at the substrate surface from gases in the ground state. The reaction progresses under nearly thermodynamic equilibrium. On the other hand, PECVD is a film formation technique that causes excited species to react with each other in the gas phase. This makes it possible to deposit films at lower substrate temperatures than with thermal CVD, in which a high substrate temperature is necessary to cross over the activation energy.

In order to generate a discharge for cold plasma, low pressure is of course required. PECVD is, however, a film formation process which includes chemical reactions. Therefore, higher particle density of active species is required in order to get higher deposition rates. The pressure range in PECVD lies between *0.1* and *10 Torr*. Mean-free path of gas particles at this pressure range are as short as several hundred micrometers [17].

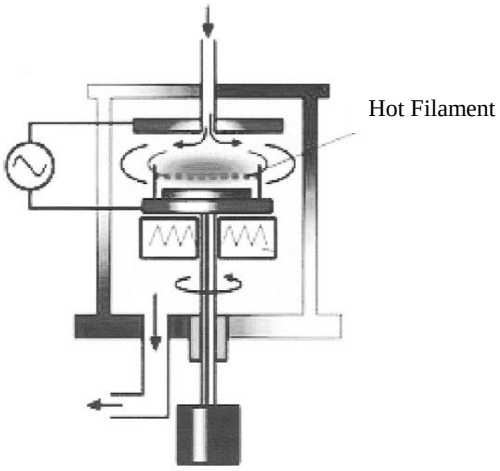

Fig. 6. *Schematic of PECVD [14]*

The growth of CNTs using PECVD is a very complicated process because it involves many determining factors in growth conditions. These important factors involve the catalytic material, the catalytic support material (namely, catalyst–substrate interactions), the growth temperature gradient across the catalytic particle and the effect of plasma. Compared with conventional CVD, plasma-enhanced chemical vapor deposition (PECVD) is advantageous for the direct growth of CNTs on the substrates at a relatively low growth temperature and also large area fabrication of CNTs due to the presence of an uniform plasma [18].

It is easier to fabricate aligned CNTs, at lower substrate temperature by using PECVD technique. Various plasma sources have been used for the growth of CNT such as microwave, direct current, and inductive coupled radio frequency. However, these sources are not suited for the large area deposition, because it is difficult to generate an uniform plasma for a large area. However, capacitive coupled radio frequency PECVD (rf-PECVD) method has a possibility for the large area deposition, because the plasma is very stable and homogeneous. However, the quality of CNT synthesized by rf-PECVD method is comparatively poor; for example, it is covered with large amount of carbon soot, it has a low aspect ratio and a stacked-cone structure [19].

C. CNTs Growth Mechanism

Quantum molecular dynamics simulations have been reported to understand the growth process of MWCNTs [20]. Within such calculations, the topmost atoms (dangling bonds) of the inner and outer edges of a bilayer tube rapidly move towards each other, forming several bonds to bridge the gap between the adjacent edges, thus verifying the assumption that atomic bridges could keep the growing edge of a nanotube open without the need of "spot-weld" adatoms.

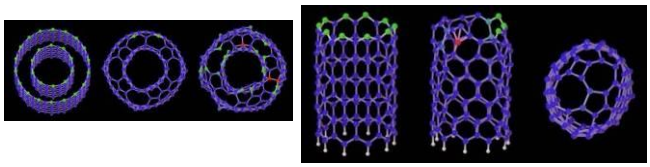

Fig. 7. *(a) Spontaneous closure of SWNTs at ~3000K (b) Open-ended growth of MWNTs stabilized by "lip-lip" interactions at ~3000K [20]*

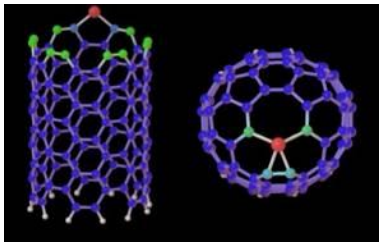

Fig. 8. *Close-ended catalytic growth of SWCNTs at ~1500K [20]*

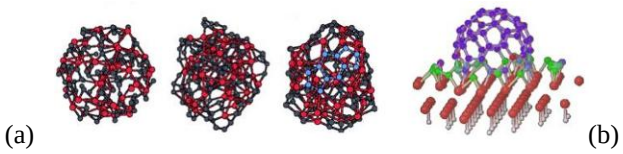

Fig. 9. *(a) First step: segregation of carbon at the nano-particle surface when cooling from 2000K to 1500K (b) Second step: nucleation and growth of a carbon nanotube germ extruding from a large catalytic nanoparticle [20].*

At *~3000K* (a typical experimental growth temperature), the "lip-lip" interactions stabilize the open-ended bilayer structure (fig.7) and inhibit the spontaneous dome closure of the inner tube as observed in analogous simulations of single-shell tubes. These calculations also show that this end geometry is highly active chemically, and easily accommodates incoming carbon clusters, supporting a model of growth by chemisorption from the vapor phase [20]. The catalytic growth of SWNTs (fig.8 & 9) was investigated using first-principles molecular dynamics simulations. At experimental temperatures (*~1500K*), even though the open end of SWCNTs closes spontaneously into a graphitic dome, the metal-carbon chemical bonds keep breaking and reforming. Such phenomenon provides a direct incorporation process for the necessary additional carbon, and suggests a close-end mechanism for the catalytic growth. The catalytic action of metallic atoms is also found to play a key role in the reconstruction of the nanotube tip after carbon incorporation, by annihilation of defects. The short range action of the metal may explain the relatively narrow diameter observed for SWCNTs [20].

The nucleation and growth of SWCNTs within a root growth mechanism (where carbon atoms precipitate from particles larger than the tube diameter) was studied using quantum molecular dynamics simulations. It was suggested that carbon atoms can be added at the root of a growing tube by a diffusion-segregation process occurring at the surface of the catalytic particle [20].

II. THE GOAL OF THESIS

The main objective of this work is to optimize the production of Carbon Nanotubes (CNTs) as base material for supercapacitors using PECVD. Therefore, we will try to maximize the surface-area characteristics and electrical properties of obtained CNTs.

In order to achieve this, several milestones should be reached:

- Optimization of the catalyst layer thickness and annealing time in order to obtain a homogenate and desired catalyst particle formation.

- Optimization of the PECVD operating parameters (reaction time and temperature) to grow dense and long CNTs.

- Optimization of the CNTs purification by means of water plasma in order to remove amorphous carbon from the CNTs samples and to open the tips of CNTs increasing their specific area.

III. EXPERIMENTAL

A. Reactor

This section explains all reaction steps with details.

CNTs production was carried out in PECVD reactor which was developed by the FEMAN group as a result of the European Project NANOTUBE. This reactor has 3 homemade magnetron sputtering heads that permit to deposit materials onto wafers without taking them out of the system. All operations are controlled with especially designed LabView software (version 7.1, National Instruments, USA). To heat the system during annealing and PECVD, Xantrex (XDC 60-100, Digital DC power supply, Canada) heater is used. As vacuum plays an important role in sputtering and PECVD processes, 3 types of pumps are used in the reactor. From atmospheric pressure to *~2 x 10^3 Pa* or lower, rotatory pump (EV25 QS AL, Laybold Vacuum GmbH, Germany) is used, from *~2 x 10^3* to *~3 x 10^{-2} Pa* Root pump (WU 251, Leybold Heraus RUVAC, Germany) and from *~3 x 10^{-2}* to *~4 x 10^{-4} Pa* Turbamolecular pump is used (Turbovac 361C, Leybold Vacuum GmbH, Germany).

a. Sample Preparation

In PECVD process, CNTs were grown onto Si wafers. These wafers are p-type boron doped Silicon (Si) and their resistivity is between *0.01* to *0.02 Ω cm^{-1}* (4482/R, SI-MAT,

Germany). They were prepared in the size of *1.5 cm* x *1 cm*. To introduce Si samples into the reactor, graphite holders were used. Another Si wafer was attached onto graphite with silver paint to obtain better thermal contact between holder and sample.

b. Sputtering

Nanometric transition metal particles (Fe, Co, Ni, Pd. . .) are indispensable to catalyze CNT growth when using PECVD methods. That has been generally done by physical vapor deposition (PVD) techniques, magnetron sputtering or patterned by electron lithography methods. Anyhow, catalyst deposition is an auxiliary step in PECVD grown CNTs [21]. In sputtering process (fig.10), magnetron was used to create magnetic field which is parallel to the cathode and plasma was generated by radio frequency which was the energy source used between anode and cathode, so it is called rf-magnetron sputtering. Fe was chosen as catalyst and Ar as precursor gas (*128 sccm*, achieving *2 Pa*), the process was operated at *50 W* (TIS 0.5/13560, Huttinger, Germany), For the first time operation of Fe target, there is need to calibrate it. This calibration was performed by depositing Fe layer during *30 min*. onto glass sample and checking its thickness in AFM. After that, by dividing this thickness to *30 min.* deposition rate of Fe target was calculated for *1 min.* and then sputtering time for process was obtained for desired Fe thickness. For the optimized conditions, *91 s* sputtering were needed to obtain a resulting *3 nm* thickness Fe layer.

c. Annealing

Annealing is a crucial step where prepared Fe layer is cracked into nanometric Fe-islands (fig.11). These nanoislands will be the origin of CNT growth and it is necessary to obtain homogenous island dispersion on wafer. In our case, Fe layer was heated up to several temperatures between *650°C* and *850°C* and kept during *2 min*. H_2 gas (Air Liquide, France) was used at *2 mbar* and *100 sccm* to keep a reducing atmosphere and avoid Fe oxidation.

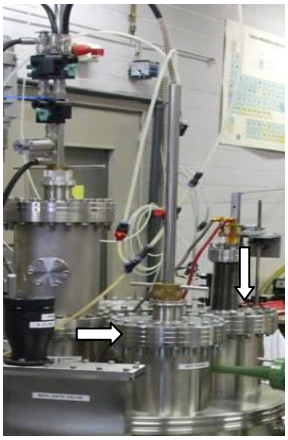

Fig. 10. *Sputtering heads*

d. Reaction (PECVD)

The special design of the reactor (fig.12) permits to send directly the wafer from annealing to reaction position. In this way, contact of Fe layer with air and its potential oxidation was prevented.

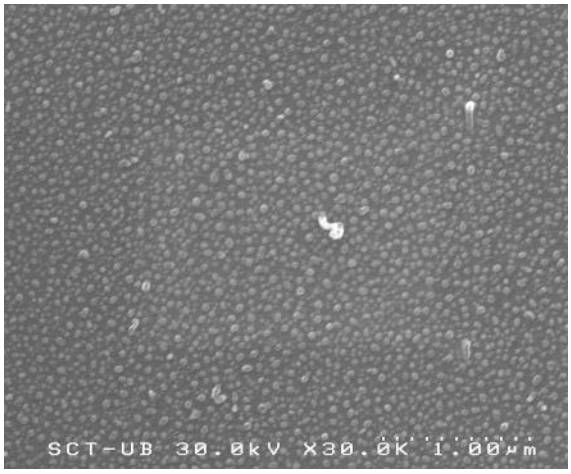

Fig. 11. *Fe layer after annealing*

Fig. 12. *Reactor: From left to right; place to introduce sample inside the chamber and 4 different heads; 2 for Fe and Si sputtering, 1 for heater and PECVD reaction and last one is free.*

Reaction parameters are shown in the table;

TABLE I.
PECVD REACTION PARAMETERS

Precursor Gas*	NH_3
Flow rate	100 sccm
Carbon Source**	C_2H_2
Flow Rate	50 sccm
Purge pressure	0.8 mbar
Reaction Pressure	1 mbar
Plasma Power	50 W
Reaction Temperature	650 to 850°C
Reaction Time	600 to 1200 s

* (Conc.99.9%, Linde, Germany) ** (Conc.99.6%, Praxair, Spain)

After obtaining an appropriate dispersion of Fe nanoislands on Si wafer, the process of CNTs growth can start. Fig.13 shows, the PECVD reaction diagram and a micrograph of the resulting CNTs.

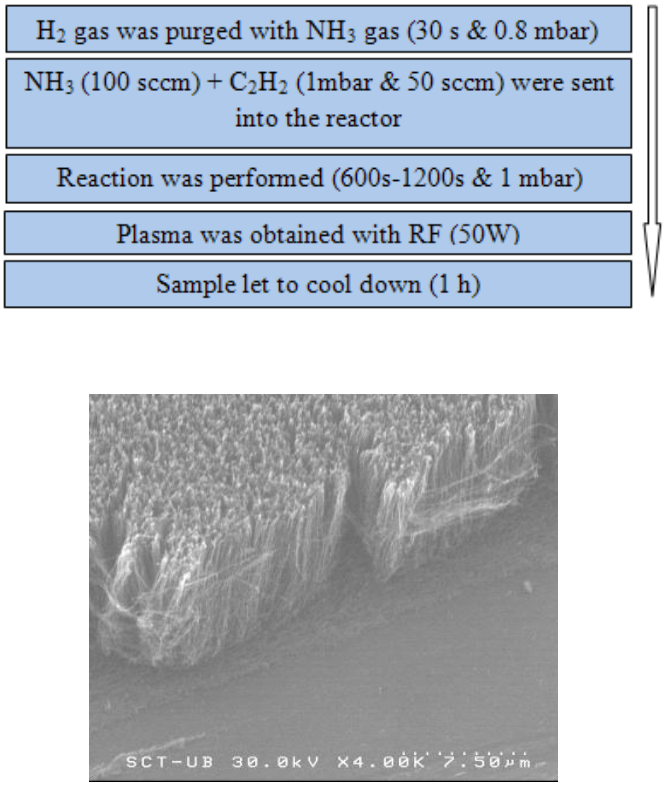

Fig. 13. *Reaction diagram and CNTs photo after PECVD*

e. Water plasma

Growth of CNTs with PECVD reaction causes the presence of amorphous carbon on the obtained CNTs and this should be removed to increase the deposit specific area of CNTs and to improve their electron transfer capability. Another advantage of water plasma application is to cut off tips of CNTs where Fe catalyst particles exist. Opening tips of CNTs would supply more surface area for applications.

This procedure was operated at *50W, 50Pa* H_2O plasma and during *30, 60* and *300 s*.

B. Characterization Methods

In this work, several characterization methods were used. In this section, a brief description was given and role of Atomic force microscopy (AFM), Transmission and Scanning electron microscopies (TEM, SEM) and Raman spectroscopy methods were explained. As well as for checking morphology of CNTs, these helpful tools were also used for some specific aims.

AFM imaging is performed by scanning a very sharp tip across the sample surface while the force of interaction between the tip and the sample is monitored at pN sensitivity. The sample is mounted on a piezoelectric scanner which ensures three-dimensional positioning with high resolution, and the force between tip and surface is monitored by measuring the cantilever deflection using an optical method (laser, photodiode) [22].

In this study we used a Park Systems XE series AFM (South Korea). During studies, non-contact mode was used to keep safe the cantilever tip and measurements were seen and interpreted with Ueye (version 2.40.0005) and XEI (version 1.7.3) software. Moreover, AFM was used to calibrate the catalyst deposition rate.

SEM is a type of electron microscope that images the sample surface by scanning it with a high-energy beam of electrons in a raster scan pattern. The electrons interact with the atoms that make up the sample producing signals that contain information about the surface topography of sample, composition and other properties such as electrical conductivity.

The signal produced by SEM includes secondary electrons, back-scattered electrons (BSE), characteristic X-rays, light (cathodoluminescence), specimen current and transmitted electrons. Secondary electron detectors are common in all SEMs, but it is rare that a single machine would have detectors for all possible signals [23].

In this work, SEM was used to check the dispersion and diameter of the Fe particles after the annealing step and to characterize the CNTs morphology. The system is HITACHI S 2300 type SEM (Japan) and it belongs to University of Barcelona's Serveis Cientifico-Tecnics (SCT-UB).

TEM is a microscopy technique whereby a beam of electrons is transmitted through an ultra thin specimen,

interacting with the specimen as it passes through. An image is formed from the interaction of the electrons transmitted through the specimen; the image is magnified and focused onto an imaging device, such as a fluorescent screen, on a layer of photographic film, or to be detected by a sensor such as a CCD camera.

TEMs are capable of imaging at a significantly higher resolution than optic microscopes, owing to the small de Broglie wavelength of electrons. This enables the instrument's user to examine fine detail—even as small as a single column of atoms, which is tens of thousands times smaller than the smallest resolvable object in an optic microscope [24].

Philips CM-30 (The Netherlands) type TEM that was used for this project belongs to SCT-UB.

Raman spectroscopy relies on inelastic scattering, or Raman scattering, of monochromatic light, usually from a laser in the visible, near infrared, or near ultraviolet range. The laser light interacts with phonons or other excitations in the system, resulting in the energy of the laser photons being shifted up or down. The shift in energy gives information about the phonon modes in the system. Typically, a sample is illuminated with a laser beam. Light from the illuminated spot is collected with a lens and sent through a monochromator. Wavelengths close to the laser line, due to elastic Rayleigh scattering, are filtered out while the rest of the collected light is dispersed onto a detector. Finally, an obtained spectrum is interpreted according to peaks and materials they belong to [25].

HORIBA Jobin Yvon T 64000 (Japan) type Raman machine that also belongs to SCT-UB, was used to check the presence of carbon and oxygen in prepared samples by PECVD and also MnO_2 deposition on CNTs which was performed to enhance the capacitance of supercapacitor.

C. Electrochemical Deposition & Characterization

This part of work was performed in AUTOLAB (89/336/EEC, Eco Chemie B.V, The Netherlands). Using this system, CNTs were coated with a MnO_2 layer which will perform as a dielectric layer in the supercapacitor. Based on a homemade experimental set up, electrochemical characterization of previously obtained CNTs samples was carried out. Capacitance behavior of samples was studied with cyclic voltammetry (CV) and obtained spectra interpreted area of samples was calculated using CV. To examine capacitance values of electrodes, charge-discharge experiment results and related formulas were used. Operational details of both the electrochemical deposition and the electrochemical characterization are included in the Mr. Toygan Mutlu's master thesis.

IV. RESULTS & DISCUSSION

A. Optimization of Annealing Time

Annealing time is a crucial parameter to obtain low diameter homogenously dispersed catalyst particles. These nanoislands of catalyst will strongly influence the characteristics of the CNTs which will grow on them. To optimize the annealing time of Fe catalyst particles, other parameters were held constant; catalyst thickness as *5 nm*, PECVD reaction time as *900 s* and reaction temperature as *750^oC.*

In annealing process, system went up to *750^oC* at different times (ramp time) and was kept at this temperature during *120 s* (hold time). Annealing time was taken as sum of these 2 values and it was assigned like; *10 min*., *14.5 min*. and *30 min*.

Using SEM pictures (fig.14) and ImageJ software (version 1.42q), mean diameter (fig.15), standard deviation and the density of Fe particles were calculated (table II). It was concluded that at *14.5 min*. annealing time, lowest Fe catalyst diameter (*32±8nm*) and homogenous dispersion of particles were obtained. Fe catalyst particles' diameters distribution is shown in (Fig.15) histogram.

At *10 min*. sample (Table II), formation of catalyst particles was not small enough (*51±10nm*). It showed that this amount of annealing time was not enough to form desired catalyst structure. At *30 min*. sample, number of nano catalyst islands was low. This probably happened because of diffusion of Fe into Si wafer after a long annealing time. Also it was observed that with increasing annealing time -between *10min* and *30 min.* - catalyst diameter increased and particle density decreased. This is due to the particle coalescence.

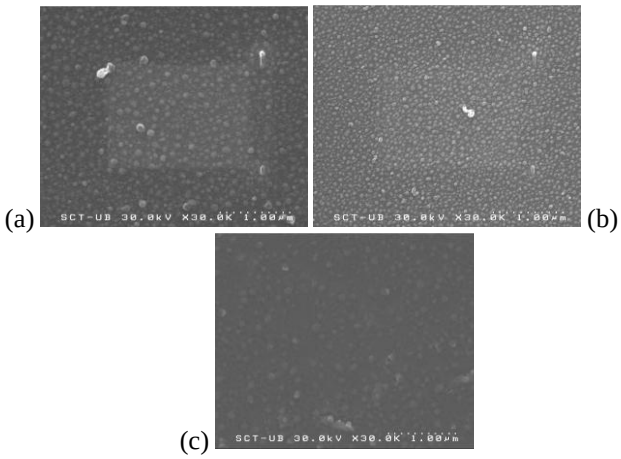

Fig. 14. *SEM pictures of (a) 10 min., (b) 14.5 min. and (c) 30 min. Annealing time (all pictures were taken at 30 kV, X30.0K and 1μm unit length)*

TABLE II
PROPERTIES OF FE CATALYST PARTICLES

Samples	Fe catalyst diameter (nm)	Fe catalyst nanoparticles (in 12 μm^2 area)
10 min.	51±10	1259
14.5 min.	32±8	3415
30 min.	83±20	913

** 12 μm^2 is the surface area which was observed by SEM. Comparison of Fe catalyst density was performed calculating mean number of particles in this unit area.*

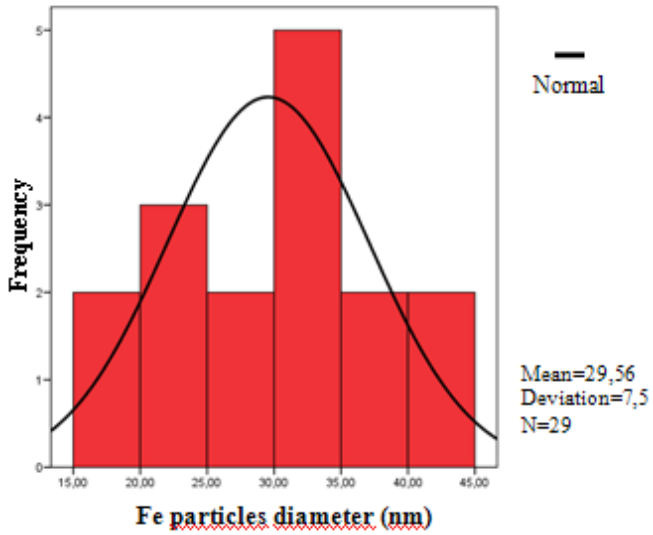

Fig. 15. *The histogram of Fe catalyst particle diameter*

B. Optimization of Catalyst Thickness & PECVD Reaction Temperature

As well as homogeneity and well dispersion of Fe catalyst, also its thickness has important role in CNTs growth. Besides this parameter, another crucial point is temperature dependence of PECVD reaction even if there is no need to reach as high temperature as in CVD process. Plasma ambient makes possible to obtain CNTs at lower temperatures.

In this case, it was decided to optimize both catalyst thickness and reaction temperature at the same time. For this, Box-Wilson experimental design was adapted for chosen parameter values. To perform experiments, 13 conditions were chosen according to Box-Wilson graph distribution (Fig.16).

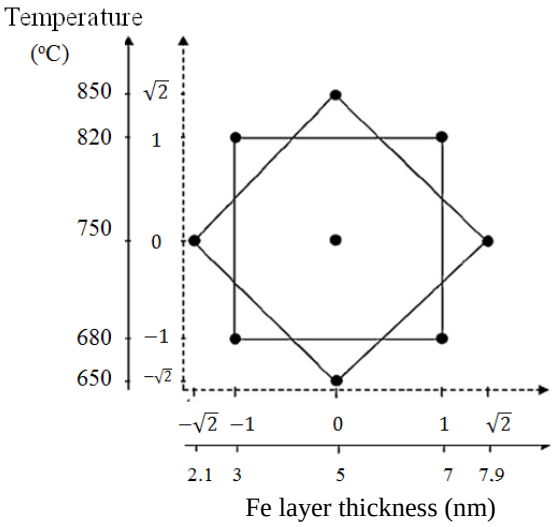

Fig. 16. *Box-Wilson experimental design samples distribution*

The use of this experimental design enables to optimize simultaneously two operating parameters taking into consideration also the possible interactions between these two parameters. The central point of the experimental design was replicated 5 times in order to evaluate the intrinsic standard deviation of the process.

In Box-Wilson design; Diameter, length, density and alignment of CNTs were evaluated as dependent variables (Table III). The goal was to obtain dense, vertically aligned long and thin CNTs. In this way, a second degree polynomial equation including the first level interactions was developed for each dependent variable:

$$Diameter = \alpha_0 + \alpha_1 T + \alpha_2 t + \alpha_3 T^2 + \alpha_4 t^2 + \alpha_5 Tt \qquad (1)$$

Where, T is the PECVD temperature, t is thickness of Fe catalyst layer and α_n are coefficients obtained by statistically adjusting these polynomial equations.

In Fig.17 we can see how temperature is significantly negatively correlated ($p<0.01$) with the density of the obtained CNTs. Therefore the denser deposits are obtained at lower temperatures. The first interaction coefficient (AB) is also significant from a statistical point of view and positively correlated with the density. After adjusting the eq. 1 we obtained the following equation:

$$Diameter = -2.8 + 0.11T - 8.5t - 0.0001T^2 + 0.06t^2 + 0.01Tt$$

This model is statistically significant ($p<0.05$) and explains *85%* of the samples variation. For some of the dependent variables the statistical correlations were not so clear and in these cases explained sample variation is lower. This is due to the high internal variation observed for the central point (between *11* to *28%* depending on the parameter) which increases the complexity of the evaluation.

Table III
SUMMARY OF THE OBTAINED EXPERIMENTAL RESULTS BASED ON SEM IMAGES TREATMENT

#	Temperature (ºC)	Fe layer thickness (nm)	CNTs diameter (nm)	Fe diameter† (nm)	Length (µm)	Density*	Alignment*
1	680	7.0	72	82	6.8	7	7.5
2	750	5.0	-**	-**	-**	-**	-**
3	820	3.0	133	100	3.6	1	0.0
4	750	5.0	95	69	2.5	5	5.0
5	849	5.0	-**	-**	-**	-**	-**
6	820	7.0	64	-**	0.5	5	0.0
7	651	5.0	72	37	3.9	7	7.5
8	750	5.0	104	90	3.8	6	5.0
9	750	5.0	93	76	5	4	2.5
10	750	2.2	-**	-**	-**	-**	-**
11	680	3.0	59	13	7.4	9	10.0
12	750	5.0	64	80	4.5	6	5.0
13	750	7.8	114	43	3.1	6	5.0

†CNT samples were locally and smoothly scratched using plastic tweezers in order to remove the CNTs and be able to observe the Fe particles lying underneath.
*Semi quantitative values evaluated from SEM images.
**Data not available, no CNTs and Fe particles present.

As an example of the statistical study we present the obtained results for the density dependent variable.

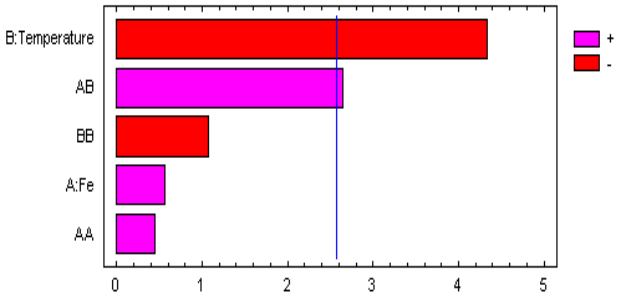

Fig. 17. *Pareto diagram of the standardized effects of the different parameters A (Fe catalyst layer thickness) and B (PECVD temperature) on the CNTs density. Blue line corresponds to p=0.05.*

Based on these results the optimal operating PECVD conditions were defined as being *3 nm* thickness Fe catalyst layer and *680ºC* PECVD temperature.

Hereafter some images of the obtained samples are presented in order to illustrate the observed intersample differences.

In fig.18, picture (a) and (b) showed that at higher catalyst thickness, CNTs become thicker (*114 nm* in diameter) and respectively shorter (*3.1 µm*). Picture (c) showed that at lower reaction temperature CNTs are short again. In fig.19, picture (d) and (e) showed that higher reaction temperature and low catalyst thickness can be reasons for poor CNTs growth. At high temperature or low catalyst thickness, Fe particles may diffuse inside the Si wafer and the surface shows not enough catalyst for CNTs growth.

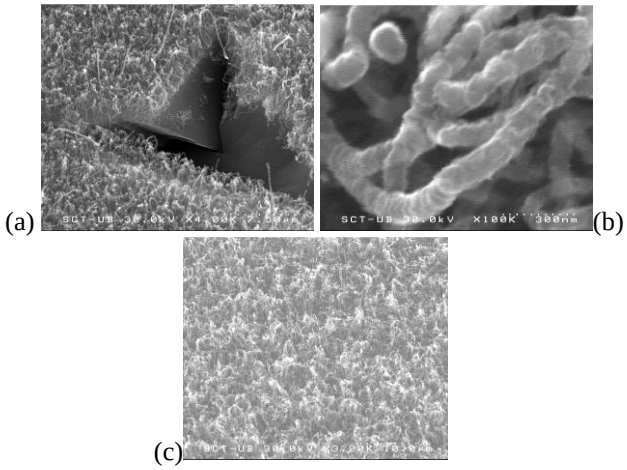

Fig. 18. *(a) & (b) 7,9 nm / 750 ºC sample, (c) 5 nm / 650 ºC sample*

Fig.20 shows that, at the same conditions, the reactor can reproduce CNTs with the same characteristics (vertical alignment and *3-4 µm* length). After the Box-Wilson experimental design three samples were grown at our selected optimum conditions. As an example, Fig. 21 shows the obtained result, long (*9.1 µm*), thin (*14 nm*) dense and vertically aligned CNTs. TEM results showed that obtained CNTs are multiwall ones and their diameter is *~20 nm*. The number of walls was determined by ImageJ (version 1.42q) the obtained CNTs are MWCNTs and have typically 27±5 walls.

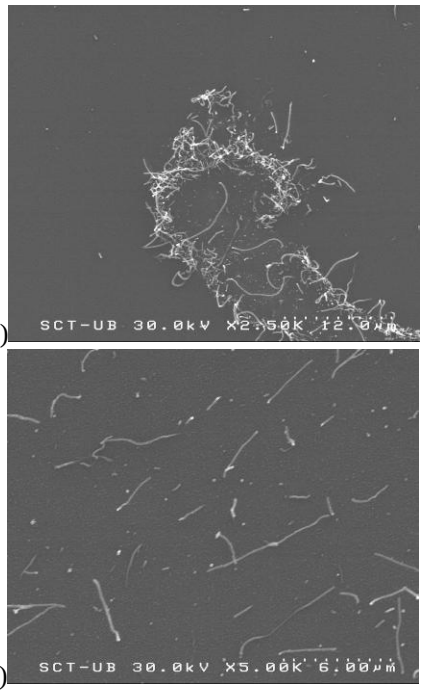

(d) (e)

Fig. 19. *(d) 2,1 nm / 750 °C sample, (e) 3 nm / 820 °C sample*

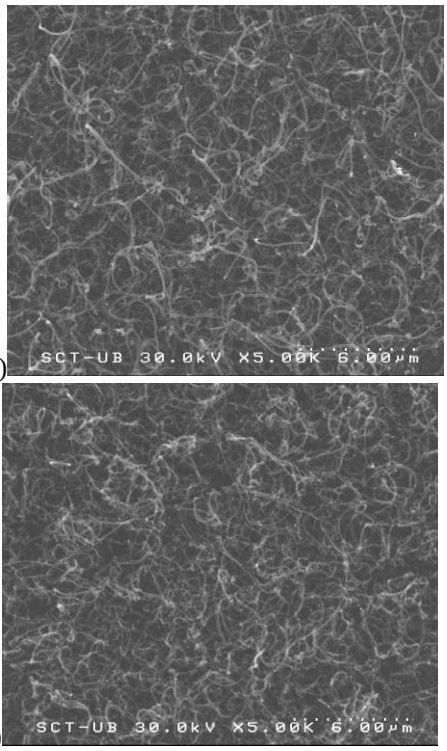

(g) (f)

Fig. 20. *(f) and (g) 5 nm / 750°C samples*

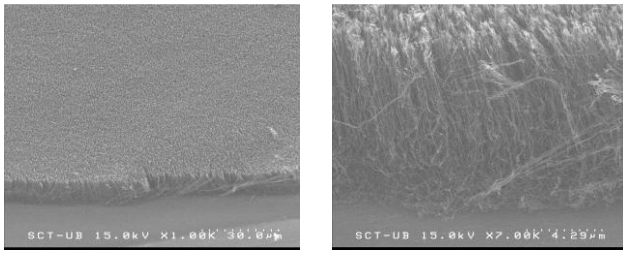

(h) (i)

Fig. 21. *(h) & (i) 3 nm / 680°C sample*

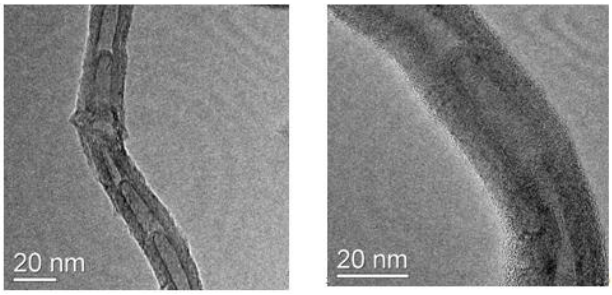

(j) (k)

Fig. 22. *(j) & (k) TEM pictures at the optimum PECVD operating conditions*

Based on these replicated samples optimum PECVD operating conditions were confirmed:
Annealing time (14.5 min), catalyst thickness (3nm) and PECVD temperature (680°C).

C. Optimization of PECVD Reaction Time

PECVD reaction time was studied at 3 different values; *600 s*, *900 s* and *1200 s* (table IV).

This trial has an interesting effect on CNTs morphology. If reaction time keeps shorter, CNTs will not reach desired length however, if deposition time is too long, length of CNTs will decrease. This fact could be explained considering that after an optimum deposition time no more active catalyst is available. Therefore, CNTs growth stops but plasma etching continues shortening CNTs length. Fig.22 shows two TEM pictures of CNTs grown at the optimum PECVD conditions.

TABLE IV
RESULTS OF PECVD REACTION TIME OPTIMIZATION

Time of PECVD (s)	Reaction Temperature/ Catalyst Thickness	Diameter of CNTs (nm)	Length of CNTs (µm)
600	680°C/3 nm	45±10	4.2±1
900	680°C/3 nm	22±9	16.9±5
1200	680°C/3 nm	30±10	9.8±1.5

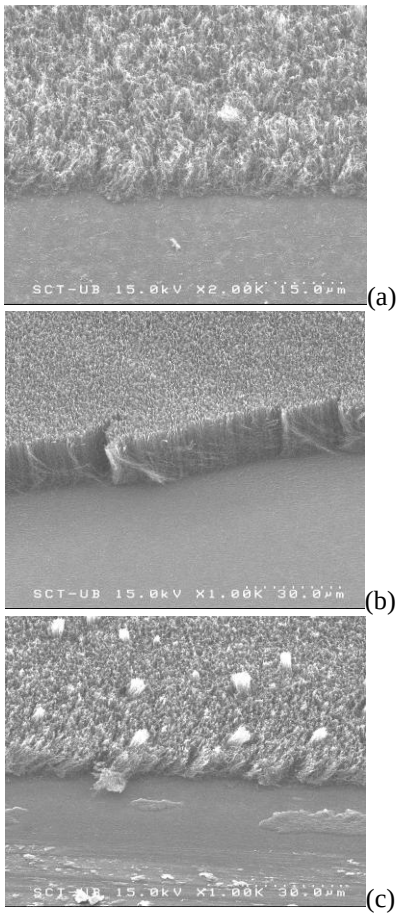

Fig. 23. *SEM pictures of (a)600s, (b)900s and (c)1200s reaction times*

SEM results (fig.23) showed that, sample (b) at *900 s* reaction time, has the best CNT length. Sample (a) at *600 s* reaction time, has shortest CNTs and worst density and thickest CNTs. Sample (c) at *1200 s* reaction time, has good density but not as long CNTs as *900 s*. This could be due to the destructive effect of long PECVD reaction time.

D. Optimization of Water Plasma Time

Natural result of growing CNTs with PECVD reaction is the presence of amorphous carbon covering the CNTs layer. This situation decreases the specific area of the material and masks the characteristic properties of the CNTs. This amorphous carbon has been removed via a water plasma oxidation step. Moreover, this step, if intense enough, could break the tip of the CNTs and in this way the inner part of the CNTs could also be used. Water plasma was applied at *50 Pa* pressure and *50 W*. To optimize it, 3 different plasma times were studied; *30 s*, *60 s* and *300s* (Table V and fig.24).

TABLE V
RESULTS OF OPTIMIZATION OF WATER PLASMA TIME

Water Plasma time (s)	Catalyst Thickness/Reaction Temperature	Lenght of CNTs (µm)	Diameter of CNTs (nm)
30	3nm/680°C	8.6±1	37±7
60	3nm/680°C	11.26±1	17±4
300	3nm/680°C	5.5±2	18±4

After water plasma treatments (fig.24), by comparing sample (c) and sample (d), it was obtained that amorphous carbon was removed from all samples. On the other hand, all samples proved that tips of some CNTs were opened however some of them are still carrying Fe particles. It means that water plasma was not intense enough to open all of their tips.

Water plasma treatment slightly affected the diameter of CNTs. This can be proved by comparing these 2 samples with and without water plasma treatment. Sample (c) and (d) of fig.24 and TEM results (fig.25) showed that while sample (a) which is without water plasma treatment, has *24±4 nm* diameter, sample (b) with water plasma treatment, has *19±4 nm* diameter. After observation with ImageJ (version 1.42q) software, the number of walls of CNTs was also decreased at *17±3* (which is *27±5* for sample without water plasma). Therefore, it could be predicted that in these conditions the removal of the amorphous carbon from the CNTs layer also affects the CNTs structure by removing the most external walls of the CNTs.

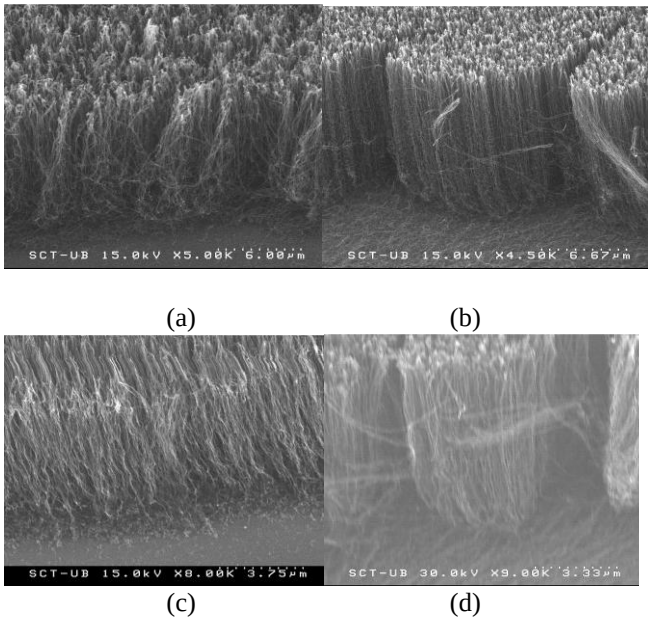

Fig. 24. *Sample (a) 30 s, sample (b) 60 s, sample (c) 300 s water plasma and sample (d) without water plasma*

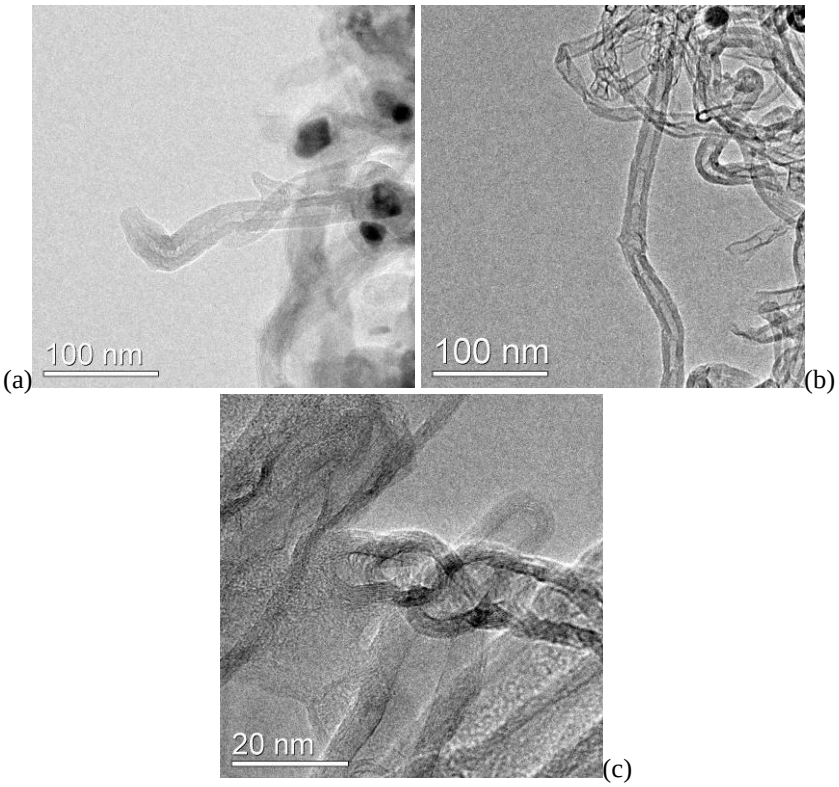

(a) (b) (c)

Fig. 25. *TEM pictures; samples (a) and (b) with water plasma treatment, sample (c)without water plasma treatment*

According to Raman application notes of HORIBA Jobin Yvon Company, which is the trademark of Raman Spectroscopy, used in this work, the weak peaks between *3100-3650 cm^{-1}* correspond to OH group and medium peaks between *1680-1820 cm^{-1}* correspond to C=O groups [26]. Oxygen containing groups might be seen after water plasma because open tips of several CNTs form bonds with oxygen that comes from the H_2O dissociation during the water plasma process. But in this work, peaks were not enough intense due to the fewness of open CNTs tips. Also, spectra (c) showed that when there is no water plasma treatment, peaks corresponding to carbon-carbon aromatic ring chains dominate this region even if they are not completely well defined. In spectra (d) it is obvious that after water plasma treatment, these peaks became more intense because of removing amorphous carbon [fig.26].

E. Optimization of MnO_2 Deposition Time

This part of the work was performed in Autolab. 3 different deposition times were tried to find the optimum MnO_2 deposition time (*3min*, *6min* and *10 min*). Comparing CV results of different deposition times, *3min.* was obtained as optimum one. At this deposition time, thickness of MnO_2 layer was found as being *2.4±0.4nm*. Detailed explanation was given in master thesis of Mr. Toygan Mutlu.

F. Results of Cyclic Voltammetry and Charge/Discharge

In electrochemical characterization, different samples were studied systematically. These are shown in table VI.

According to these results, if interpretation is done respectively; dense aligned CNTs have higher active surface area than relatively less dense one. It is logical that when there are more CNTs on electrode, the active surface area increases. The decrease in active surface area observed when CNTs are treated with water plasma may be due to the material removal caused by this oxidation step. Depositing MnO_2 onto the CNTs with water plasma treatment lost some of the pores present in the CNTs layer and resulted in a decrease in active surface area.

The difference in specific capacitance of dense CNTs and relatively less dense CNTs is not so different, but the effect of water plasma treatment in specific capacitance can be easily seen as nearly 5 times higher than dense CNTs. This is the result of removing amorphous carbon and therefore the improvement of the electrical characteristics of the CNTs layer. Finally, MnO_2 deposited CNTs which have dielectric material between them, showed higher specific capacitance. In this way, the obtained result (463 F/g) was compared with bibliography and it is close to other reported values [27]. However, these results could be improved in a short time

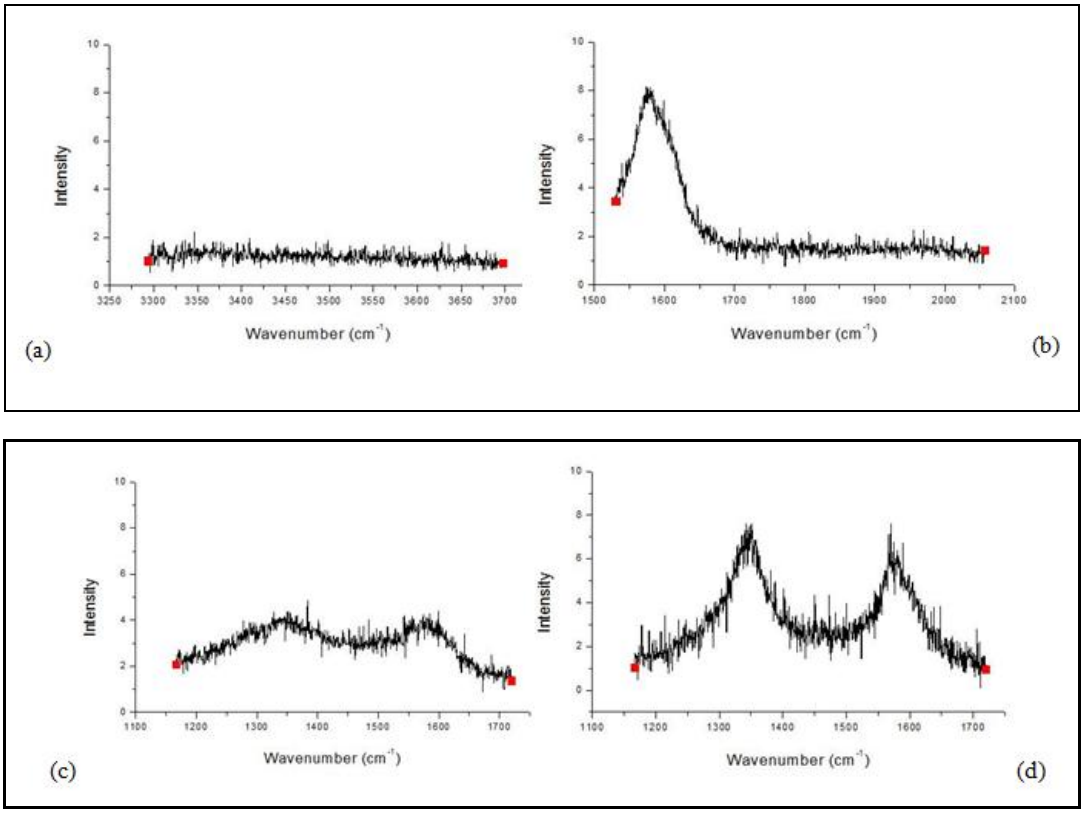

Fig. 26. *Raman Spectrum of (a),(b),(d with water plasma and (c)without water plasma treatment*

TABLE VI
SPECIFIC AREA & SPECIFIC CAPACITANCE OF SAMPLES

Samples	Immersed Area (cm^2)	Active Surface Area (cm^2)	Active Surface Area/Immersed Area	Specific Capacitance (mF/cm^2)
Si wafer	not available	not available	not available	not available
Si wafer + CNTs	1.43	1.04±0.02	0.72	0.11
Si wafer + CNTs (dense-aligned structure)	0.64	3.92±0.1	6.125	0.19
Si wafer + CNTs + Water plasma treatment	0.49	1.04±0.02	2.12	1
Si wafer + CNTs + Water plasma treatment + MnO_2 deposition	0.55	0.36±0.02	0.65	4.5 (463 F/g)

because of the new knowledge about the capacitance behavior of CNTs layers acquired during this master thesis.

V. CONCLUSION

- By using specially modified PECVD reactor by FEMAN group of the Applied Physics and Optics Department, CNTs were obtained to make electrodes for supercapacitor applications. These CNTs have diameters as low as *14 nm* and length as long as *13 μm*.
- Si was chosen as substrate, Fe was the catalyst which was deposited by rf-magnetron sputtering and water plasma treatment was carried out after PECVD reaction to remove amorphous carbon from the CNTs samples.
- To obtain best design parameters, optimization was done for all these steps; annealing time, catalyst thickness, reaction time and temperature and water plasma time. According to this work, *3nm* Fe catalyst thickness, *14.5 min* annealing time, 680^oC temperature for annealing and reaction and *60 s* for water plasma treatment were obtained as optimum conditions. All these steps were assessed with SEM, TEM and Raman spectroscopy techniques.
- Optimum deposition time of MnO_2 was obtained as *3 min*. Deposition thickness of MnO_2 onto CNTs was *2.4±0.4nm*.
- These obtained electrodes were characterized with electrochemical methods like CV and Charge/Discharge to see their supercapacitor properties.
- Finally, these characterization results showed that MnO_2 deposited Si-based MWCNTs electrode achieved *0.36* cm^2 active surface area and *463 F/g* specific capacitance.

It was proved that PECVD is a strong and robust method to grow CNTs for electrodes to use them in supercapacitors.

VI. FUTURE ADVICE

- In this work, annealing and PECVD reaction temperatures, due to software configuration, have to be the same. It means that, when system reaches desired temperature for annealing, it is kept there several minutes and then reaction starts at the same temperature. Instead of this, by making related changes in the software program which controls all reactions, different annealing and PECVD reaction temperatures may be tried. Thereby, improved catalyst formation may be obtained at low annealing temperatures and also reaction temperature might be increased in order to improve the kinetics of CNTs growth.
- Fe was the used catalyst to obtain CNTs but according to bibliographic resources, Ni and Co are also used commonly in PECVD to grow CNTs. Instead of Fe catalyst, these other metals may be deposited on Si wafer to check if they are more active than Fe particles or not.
- Porous nickel foams are in high demand for applications in lithium ion batteries and electrochemical supercapacitors. In the batteries and supercapacitors, nickel foams are used as high surface area current collectors, containing highly accessible active material within their conducting light weight web, which provides structural strength [28]. Because of this, Si wafer which was used as both substrate and current collector could be replaced by Ni foam. Also, Ti or Au with their better conductivity may be preferred instead of silicon. However, in these cases a diffusion barrier should be deposited on the substrates in order to avoid the catalyst diffusion.
- For the deposition of MnO_2 onto CNTs, thinner MnO_2 layer may be preferred in order to avoid the decrease in the porous structure of the CNTs layer. In the same way a less dense CNTs structure may be selected to make the CNTs interspaces available to MnO_2. In some cases, only over and side walls of CNTs are covered and this prevents the entrance of electrolyte in every place and obtaining higher specific capacitance results.

ACKNOWLEDGEMENT

B. Caglar thanks to Prof. Enric Bertran, Dr. Eric Jover Comas, Dr. Roger Amade Rovira and Dr. Carles Corbella Roca for their guidance and helps in every step of this work, Serveis Científico-Tècnics of the Universitat de Barcelona (SCT-UB) for measurement facilities and colleague Toygan Mutlu for his collaboration. This work was supported by the Generalitat de Catalunya (Projects 2005SGR00666 and 2009SGR00185) and the MEC of Spain (Projects DPI2006-03070 and MAT2009-14674-C02-01).

REFERENCES

[1] http://www.nanoscience.gatech.edu/zlwang/research/nano.html
[2] http://www.nano.gov/html/facts/nanoapplicationsandproducts.html
[3] http://nanogloss.com/nanotechnology/the-potential-disadvantages-of-nanotechnology/
[4] M. Paradise, T. Goswami, "*Carbon nanotubes – Production and industrial applications*," Materials and Design, **28**, 1477–1489, 2007.
[5] V. N. Popov, "*Carbon nanotubes: properties and application*," Materials Science and Engineering, R **43**, 61–102, 2004.
[6] A. A. Shvedova, E. R. Kisin, D. Porter, P. Schulte, V. E. Kagan, B. Fadeel, V. Castranova, "*Mechanisms of pulmonary toxicity and medical applications of carbon nanotubes: Two faces of Janus?*" Pharmacology & Therapeutics, **121**, 192–204, 2009.
[7] R. Hodson, L. Hodson, "*Approaches to Safe Nanotechnology: Managing the Health and Safety Concerns Associated with Engineered Nanomaterials*," National Institute for Occupational Safety and Health (DHHS) Publication, **125**, 2009.
[8] C. A. Poland, R. Duffin, "*Carbon nanotubes introduced into the abdominal cavity of mice show asbestos-like pathogenicity in a pilot study*," Nature Nanotechnology, **3**, 423, 2008.
[9] Q. Zeng, Z. Li, Y. Zhou, "*Synthesis and Application of Carbon Nanotubes*," Journal of Natural Gas Chemistry, **16**, No. 3, 235-246, 2006

[10] J. M. Boyea, R. E. Camacho, S. P. Turano, W. J. Ready, "*Carbon Nanotube-Based Supercapacitors: Technologies and Markets*," Nanotechnology Law & Business, 2007.
[11] http://img.alibaba.com/photo/11162094/super_capacitor_Ultra_capacitor_edlc.jpg
[12] E. Frackowiak, K. Jurewicz, K. Szostak S. Delpeux, F. Beguin, "*Nanotubular materials as electrodes for supercapacitors*," Fuel Processing Technology, **77–78**, 213–219, 2002.
[13] G. X. Wang, B. L. Zhang, Y. Zuo-Long, Q. Mei-Zhen, "*Manganese oxide/MWNTs composite electrodes for supercapacitors*," Solid State Ionics, **176**, 1169–1174, 2005.
[14] A. Govindaraj, C. N. R. Rao, "*Synthesis, growth mechanism and processing of carbon nanotubes*," Carbon Nanotechnology, 2006.
[15] http://www.fy.chalmers.se/atom/research/nanotubes/images/thermal.
[16] M. Daenen, "*The Wondrous World of Carbon Nanotubes -a review of current carbon nanotube technologies-*" Eindhoven University of Technology, 2003.
[17] M. Konuma, "*Film deposition by plasma techniques*," Springer-Verlag, 1992.
[18] J. Jiang, T. Feng, X. Cheng, L. Dai, G. Cao, B. Jiang, X. Wang, X. Liu, S. Zou "*Synthesis and growth mechanism of Fe-catalyzed carbon nanotubes by plasma-enhanced chemical vapor deposition*," Nuclear Instruments and Methods in Physics Research, **B244**, 327–332, 2006.
[19] Y. Yabe, Y. Ohtake, T. Ishitobi, Y. Show, T. Izumi, H. Yamauchib, "*Synthesis of well-aligned carbon nanotubes by radio frequency plasma enhanced CVD method*," Diamond and Related Materials, **(13),** 1292–1295, 2004.
[20] http://sites.uclouvain.be/pcpm/themes/GROWTH_NT.php
[21] T. M. Minea, S. Point, A. Gohier, C. Godon, F. Alvarez, "*Single chamber PVD/PECVD process for in situ control of the catalyst activity on carbon nanotubes growth*," Surface & Coatings Technology, **200**, 1101–1105, 2005.
[22] P. Hinterdorfer, Y. F. Dufrêne, "*Detection and localization of single molecular recognition events using atomic force microscopy*," Nature Methods, **3**, No.5, 2006.
[23] http://en.wikipedia.org/wiki/Scanning_electron_microscope
[24] http://en.wikipedia.org/wiki/Transmission_electron_microscopy
[25] http://en.wikipedia.org/wiki/Raman_spectroscopy
[26] www.horiba.com/fileadmin/uploads/Scientific/Documents/Raman/bands.pdf
[27] K. V. Nam, C. W. Leea, X. Q. Yangb, B. W. Choc,W. S. Yoond, K. B. Kima, "*Electrodeposited manganese oxides on three-dimensional carbon nanotube substrate: supercapacitive behaviour in aqueous and organic electrolytes*" Journal of Power Sources **188**, 323–331, 2009.
[28] J. Li, Q. M. Yang, I. Zhitomirskya, "*Nickel foam-based manganese dioxide–carbon nanotube composite electrodes for electrochemical supercapacitors*," Journal of Power Sources, **185**, 1569–1574, 2008.